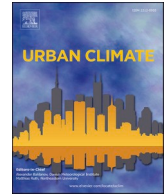




ELSEVIER

Contents lists available at [ScienceDirect](https://www.sciencedirect.com)

Urban Climate

journal homepage: www.elsevier.com/locate/uclim

Spoilt for choice - Intercomparison of four different urban climate models

Moritz Burger^{a,b,*}, Moritz Gubler^{a,b,c}, Achim Holtmann^d, Stefan Brönnimann^{a,b}

^a Oeschger Centre for Climate Change Research, University of Bern, Bern, Switzerland

^b Institute of Geography, University of Bern, Bern, Switzerland

^c Institute for Lower Secondary Education, Bern University of Teacher Education, Bern, Switzerland

^d Chair of Climatology, Institute of Ecology, Technische Universität Berlin, Berlin, Germany

ARTICLE INFO

Keywords:

Urban climate modeling
Urban planning
Urban air temperature variability
Low-cost air temperature network
Validation

ABSTRACT

In recent years, different models to simulate urban climate variables have been applied to various cities. As the model outputs are usually validated individually, this raises the question about which urban climate model to choose for what specific purpose. The present study aims to find answers to this by intercomparing air temperature outputs of four different urban climate models that have been applied in the city of Bern, Switzerland. This includes a geostatistical land use regression model and the numerical models MUKLIMO_3, PALM, and FITNAH 3D. Using data from 70 stations of an urban air temperature measurement network, we intercompare the four models by focusing on the modeled urban air temperature variability. MUKLIMO_3 outputs show a weak urban air temperature variability, while strong small-scale temperature gradients are modeled by FITNAH 3D. PALM outputs are the only ones that reproduce the impact of a large-scale ventilation pattern, but have a large positive bias. The most accurate estimates of the urban air temperature variability are obtained from the land use regression model. For future applications of urban climate models, we reinforce the need of validation with in-situ measurements, since the outputs (and subsequent policies) depend substantially on the selection of the model.

1. Introduction

One of the most important burdens of the already heated up atmosphere is the increasing risk concerning human health, which is causing an enhanced heat-related mortality across all continents (Vicedo-Cabrera et al., 2021). Higher temperatures also negatively impact mental health (Bundo et al., 2021) and labor productivity (García-León et al., 2021), and particularly affect urban areas which experience even higher temperatures, due to the urban heat island (UHI) effect (Oke et al., 2017). Since the number of people living in cities is continuously rising, heat-related risks are affecting an increasing amount of people (UN (United Nations), Department of Economic and Social Affairs, Population Division, 2019).

To apply urban heat mitigation and adaptation policies, detailed information about the prevailing temperature distribution is needed to identify particularly affected urban areas (Mishra et al., 2015). This information can only poorly be retrieved from official measurement station data, since only few of these exist in urban areas due to high costs and inappropriate siting conditions (Muller

* Corresponding author at: Oeschger Centre for Climate Change Research, University of Bern, Bern, Switzerland.

E-mail address: moritz.burger@unibe.ch (M. Burger).

<https://doi.org/10.1016/j.uclim.2024.102166>

Received 1 December 2023; Received in revised form 20 September 2024; Accepted 7 October 2024

Available online 12 October 2024

2212-0955/© 2024 The Authors. Published by Elsevier B.V. This is an open access article under the CC BY license (<http://creativecommons.org/licenses/by/4.0/>).

et al., 2013; WMO (World meteorological organization), 2021). The approach of modeling the atmospheric conditions in urban areas has thus been intensively investigated, which resulted in a substantial progress in the development and the performance of urban climate models (UCMs) throughout the last years (Geletič et al., 2021). Subsequently, various UCMs (differing by their structure, complexity, spatiotemporal resolution, and computational effort) have been applied to cities around the world to model, among other variables, the intra-urban air temperature variability (e.g. Erlwein et al., 2021; Geletič et al., 2021; Resler et al., 2021; Hürzeler et al., 2022; Vogel et al., 2022).

Since the modeling of urban climates is complex and subject to resulting uncertainties, validation of the model outputs with in-situ data is crucial (Rizwan et al., 2008; Geletič et al., 2021). To do so, data originating from official stations (e.g. Vogel et al., 2022), from short-term (mobile) measurement campaigns (e.g. Erlwein et al., 2021; Geletič et al., 2021; Resler et al., 2021), from specific urban air temperature networks (Hürzeler et al., 2022), or from citizen weather stations (van der Linden et al., 2023) may be used. However, intercomparing different UCMs remains challenging, since they are usually applied to different study areas with varying input data and specific research purposes. The decision of research institutes, city administrations, or private companies to select a specific UCM for a given study area, budget, or research focus is thus complex.

In the city of Bern, Switzerland, four UCMs have been applied in the recent years. A geostatistical land use regression (LUR) model and the numerical model MUKLIMO_3 (hereafter referred to as MUKLIMO) were run by the University of Bern (Burger et al., 2022; Hürzeler et al., 2022), while the numerical models PALM and FITNAH 3D (hereafter referred to as FITNAH) were set up by private companies (Meteotest AG and GEO-NET Umweltconsulting GmbH). The different stakeholders used varying model domains, study periods, and spatiotemporal resolutions, which results in a complex situation for end user / practitioners being not familiar with different UCMs. The aim of the present study is to shed light on this challenge by intercomparing the mutual output variable of these UCMs (nighttime air temperatures) and validating it based on data from 70 air temperature measurement stations in Bern (Gubler et al., 2021). We discuss the input data needed and examine advantages, limitations as well as use cases of the individual models to provide a reference point for researchers, city administration, or private companies searching for an appropriate model for a specific use case.

2. Methods

2.1. Study area

The present study is conducted in the city of Bern, Switzerland, which is a medium sized central European city with 140'000 inhabitants in the central urban districts and approximately 100'000 in the adjacent surroundings (Bundesamt für Statistik (BFS), 2022). The focus of this study is set on the overlapping model domain of PALM, LUR and FITNAH (Fig. 1) covering an almost quadratic (9.42 × 9.49 km) area of 89 km². Almost three quarters of that area is covered by vegetation, which can be grouped into agricultural areas,

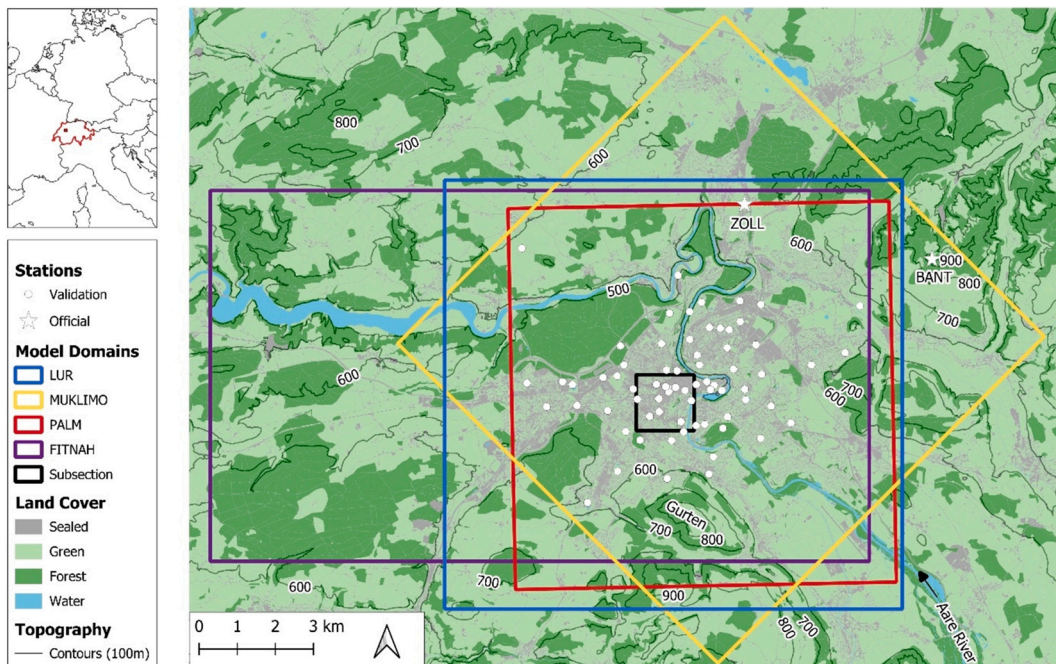


Fig. 1. Study area including the domains of the four models, land use, topography, as well as the location of the 70 validation stations (dots), and the two official stations (stars). Additionally, the location of the study area in Switzerland and central Europe is shown in the upper left corner. The black square shows a subsection that is additionally selected for a small-scale analysis.

(30 % of the study area, located mostly at the edge of the perimeter), urban forests (25 %) and small-scale green urban areas (20 %). Additionally, around 3 % of the perimeter is covered by water, mainly due to the river Aare, which crosses the city of Bern from southeast to northwest (Fig. 1). The topography is rather complex, with a maximum elevation of 858 m (Gurten hill, in the South), a minimum elevation of 481 m (in the northwest), and a mean elevation of 572 m. Approximately 22 % of the area is sealed, with an urban density that increases from the edges towards the center of the investigated area. The average building height is 14.6 m, with the tallest building reaching almost 100 m (Bernese cathedral, located in the city center).

2.2. Urban air temperature data

We use data of 70 stations of the dense urban air temperature measurement network implemented in 2018 for the validation and the intercomparison of the models. The measurement network was operated by the University of Bern and consisted of self-built, low-cost, passively ventilated measurement devices. The performance of the stations was evaluated in summer 2018 and showed, during night (22:00 to 06:00 CEST), a relatively small mean bias of -0.12 to $+0.23$ K and a root mean square error (RMSE) of 0.19 to 0.34 K, when compared to three professional, actively ventilated measurement devices (Gubler et al., 2021).

2.3. Urban climate models

Since the models were not run for the purpose of the present study, we do not explain the general setup of the models in detail, but focus on their configuration for the case study of Bern. However, basic literature, as well as baseline studies are indicated in Table 1.

2.3.1. LUR

LUR (Land Use Regression) is a geostatistical interpolation technique to model a measured response variable (here: air temperature) with a set of different spatial variables aiming for an estimation of the response variable in areas where no measurements are available (Jerrett et al., 2005). The spatial variables are calculated for different circular areas of influence (buffers), which indicate whether a variable has only a nearby or a wide-ranging effect on the response variable (Burger et al., 2021). This method was originally applied in air pollution studies (Hoek et al., 2008), but has recently been introduced to estimate urban air temperatures, due of the establishment of different urban air temperature measurement networks (e.g. Foissard et al., 2019). For this study, the high-resolution dataset of nighttime air temperatures in Bern is used (Burger et al., 2024).

2.3.1.1. Spatial input data. The study area of the LUR covers $11.45 \text{ km} \times 10.7 \text{ km}$ in a $50 \times 50 \text{ m}$ raster. For the computation of the dataset, 15 spatial variables were tested, of which seven were used in the final model: Built-up areas, forested areas, garden areas and agricultural areas (all as % of the total area), vegetation height and altitude difference to the official station (ZOLL; m) and the topographic position index, which contains information about a cell being located in a convex (+) or concave (-) position. Every raster cell thus contains information of these seven variables with varying buffer radii (Burger et al., 2022; Table S1).

Table 1
Overview of the most important features of the models used here.

	LUR	FITNAH	MUKLIMO	PALM
Model type	Geostatistical model	Computational fluid dynamic model (CFD)	Computational fluid dynamic model (CFD)	Computational fluid dynamic model (CFD)
Modeled height above surface	3 m	2 m	3 m	5 m
Study Area	122.5 km ² (11.45 km × 10.7 km)	168.1 km ² (17.29 km × 9.73 km)	146.4 km ² (12.1 km × 12.1 km; rotated by 45°)	100 km ² (10 km × 10 km; child domain) / 900 km ² (30 km × 30 km; parent domain)
Study period	2007 to 2022, every night during summer	An artificial average heat night, 21:00 to 14:00 CEST	Three heatwaves in 2018 and 2019	30.07.2018, 14:00 to 31.07.2018, 08:00 CEST
Temporal resolution	Nighttime mean (22:00 to 06:00 CEST)	04:00 CEST (hourly average)	hourly	10 min
Temperature output data used in this study	Nighttime mean, night of 30.07.2018	04:00 CEST, artificial night	Nighttime mean and early morning temperature, night of 30.07.2018	Nighttime mean and early morning temperature, night of 30.07.2018
Spatial resolution	50 m	5 m	50 m (core) to 200 m (boundary)	10 m (child) 50 m (parent)
Meteorological input data	Station data (ZOLL)	(artificial) station data (ZOLL)	Station data (ZOLL and BANT)	COSMO-1
Exchange with boundary conditions	No	Yes	No	Yes
Buildings resolved	No	Yes	No (porous medium approach)	Yes
Source	Burger et al. (2024)	GEO-NET (2023)	Hürzeler et al. (2022)	Metetest (no publication)
Model description reference	Burger et al. (2022)	Gross (1992) and GEO-NET (2023)	Sievers (2012) and Sievers (2016)	Maronga et al. (2020)

2.3.1.2. Meteorological input data. As meteorological input data, station data from the official measurement station in Bern-Zollikofen (ZOLL; Fig. 1) is used: mean nighttime air temperature (in °C), mean global solar radiation during the day (Wm^{-2}), mean nighttime wind speed (ms^{-1}) and direction (grouped in north or south) and a Boolean nighttime precipitation index (0 for 0 to 0.2 mm; 1 for ≥ 0.3 mm; Burger et al., 2022; Table S2).

2.3.2. FITNAH

FITNAH (Flow over Irregular Terrain with Natural and anthropogenic Heat sources) is a three-dimensional, non-hydrostatic model that can be used to study various parameters of the urban atmosphere. The model was developed in 1990 at the Technical University of Darmstadt (Gross, 1992), and then continuously refined by the private company GEO-NET Umweltconsulting GmbH. The model has been applied in various cities in Germany and Switzerland, such as in Zurich (GEO-NET, 2018) or Geneva (GEO-NET, 2020). Usually, daytime physiological equivalent temperatures at 14:00 CEST and nighttime air temperatures and cold air flow volumes at 04:00 CEST (hourly average) are presented and discussed by GEO-NET, mostly for a present and a future scenario. For this study, we analyze the nighttime air temperature output at 04:00 CEST for Bern that was modeled by GEO-NET on behalf of the city administration of Bern (GEO-NET, 2023).

2.3.2.1. Spatial input data. The study area of FITNAH covers the entire area of the city of Bern and the most populated parts of the adjacent communities in a 5×5 m raster. Every raster cell contains information about topography (height, slope, aspect), land use (grouped in 10 categories), height of the structure (building or vegetation) and the degree of sealing (Table S1).

2.3.2.2. Meteorological input data. FITNAH models an artificial ideal day. This is a meteorological situation with no clouds and negligible winds. In such situations, the urban atmosphere of a city is dominated by its microclimatic characteristics such as cold air drainage originating from (large) green spaces or from topographic features within the city (GEO-NET, 2023). For the case study of Bern, the meteorological variables were set the following: Relative humidity of 50 %, cloud-free sky, maximum solar radiation (21st of June), no overlying geostrophic wind, and air temperature of 21.7 °C at 21:00 CEST at the official station ZOLL (Table S2; GEO-NET, 2023). These meteorological preconditions represent a typical hot day (max air temperature ≥ 30 °C) in Bern during summer. Additionally, the model domain of Bern is nested in a $100 \text{ m} \times 100 \text{ m}$ FITNAH model covering entire Switzerland, which allows the exchange of meteorological variables (mainly wind) at the domain boundary (Table S2).

2.3.3. MUKLIMO

MUKLIMO 3 (3-dimensionales Mikroskaliges Urbanes KLimaMOdell) is a three-dimensional, non-hydrostatic model that can be used to model different atmospheric variables such as air temperature, humidity and the wind field in urban areas (Oswald et al., 2020). The model was developed by the German Meteorological Service in 1986, and continuously extended and improved since then (Sievers, 2016). MUKLIMO has been applied to analyze UHI patterns in many different cities in Europe (e.g. Bokwa et al., 2019; Oswald et al., 2020). For the present study, we use the simulation of Hürzeler et al. (2022), who modeled three heatwaves in 2018 and 2019 in the city of Bern using the MUKLIMO version v200629. In that study, a porous medium approach to model the air flow was applied in order to reduce the computational effort of modeling an entire city during three heatwaves (Table 1). This means that the air flow of every grid cell in the built-up area was parameterized using the building density, height and wall area of the unresolved buildings (Sievers, 2016; Hürzeler et al., 2022).

2.3.3.1. Spatial input data. Unlike the other models, an irregular grid was used for the MUKLIMO modeling. Starting with $50 \text{ m} \times 50 \text{ m}$ in the core area, the spacing of grid cells increases continuously to 200 m at the boundary of the modeled area (Hürzeler et al., 2022). Every grid cell contains information about the height above sea level, the fraction of impervious surfaces, and the height of buildings and vegetation. Additionally, every cell is assigned to one of 22 land use classes (Table S1; Hürzeler et al., 2022).

2.3.3.2. Meteorological input data. Every day of the simulated heatwaves was modeled individually, starting at 07:00 CEST until 08:00 CEST the next day. The first hour was used to create steady-state profiles of the atmospheric and ground variables, and was later removed (Hürzeler et al., 2022). A model run can be distinguished in two phases: First, the initial boundary conditions for every hour are calculated with given meteorological input variables (1D model). Then, the actual (3D) models starts, with the 1D model still running to provide the upper boundary values (Sievers, 2016; Hürzeler et al., 2022). For the start of the 1D model, soil temperatures at 1 m depth, soil moisture, air temperatures and relative humidity at two different altitudes (at 07:00 CEST), water temperatures, temperatures inside buildings and the cloud cover were specified. Additionally, wind speed and direction were defined for every hour of the model run (Table S2). Air temperature, humidity, wind and cloud cover data were taken from the official measurement stations ZOLL and BANT, the latter being located at a hilltop northeast of Bern (Fig. 1). Temperature measurements of the river were used to estimate the water temperature and the temperature inside buildings was fixed at 25 °C. Soil temperatures were only available at 0.5 m for ZOLL and had to be estimated based on these values. Finally, soil moisture was set to 2 on a 1 to 6 scale (Hürzeler et al., 2022).

2.3.4. PALM

PALM (originally PArallellized Large-eddy Simulation Model) is a fortran-based code that has been applied to model different atmospheric and oceanic boundary layers in the last 20 years (Maronga et al., 2015). The model has been continuously developed, and with the release of model system 6.0, components to model urban environments have been included (PALM for urban applications,

PALM-4 U), which enabled the simulation of various meteorological variables in urban environments (Maronga et al., 2020). PALM uses large eddy simulation techniques to resolve a large share of the turbulence energy, which reduces the dependence on parameterizations, but leads to an enhanced need of computational resources (Heus et al., 2010; Maronga et al., 2020). PALM has not only been applied and validated scientifically in different cities in Europe (e.g. Resler et al., 2021; Vogel et al., 2022; van der Linden et al., 2023), but has also been introduced as basis for urban heat mitigation plans in Swiss cities (such as St. Gallen) by the private company Meteotest AG (Meteotest, 2020). For this study, we use PALM (version 6.0 Rev.: 4901 M) modeling outputs for Bern that were provided by the private company Meteotest on behalf of the University of Bern.

2.3.4.1. Spatial input data. For the model setup of PALM, so-called static (for spatial data) and dynamic (for temporal data) drivers are needed (Maronga et al., 2020). Regarding the static driver, information about topography, buildings, vegetation and land use are defined for every grid cell in a file in netCDF format (Table S1). PALM offers a nested domain approach in which a parent domain exchanges boundary conditions with one or more child domains. In Bern, the parent domain covered an area of $30 \text{ km} \times 30 \text{ km}$ with a resolution of 50 m, and the child domain an area of $10 \text{ km} \times 10 \text{ km}$ with a resolution of 10 m (Table 1). In this study, we only analyze the outputs of the child domain.

2.3.4.2. Meteorological input data. The release of PALM model system 6.0 enabled the use of data from mesoscale atmospheric models as boundary conditions of the parent domain (Maronga et al., 2020; van der Linden et al., 2023). With the pre-processing tool INIFOR, COSMO-1 weather forecast simulations, provided by MeteoSwiss, were included as dynamic driver in the model (Maronga et al., 2020). The boundary conditions of the parent domain were thus updated at every time step (10 min) with COSMO-1 data which contains information about air temperature, specific humidity, soil temperature, soil moisture, wind components, surface pressure as well as geostrophic wind. Furthermore, temperatures inside buildings are directly modeled by PALM. Finally, direct measurements at the river Aare were used to set the water temperature (Table S2).

2.4. Study period and design

Although all four models were run for the same study area with very similar spatial input data (Table S1), an intercomparison remains challenging due to the differing output data. First, it is not possible to compare the same time of day of all models. We thus analyze two different time periods: nighttime mean (22:00 to 06:00 CEST, for LUR, MUKLIMO and PALM) and early morning

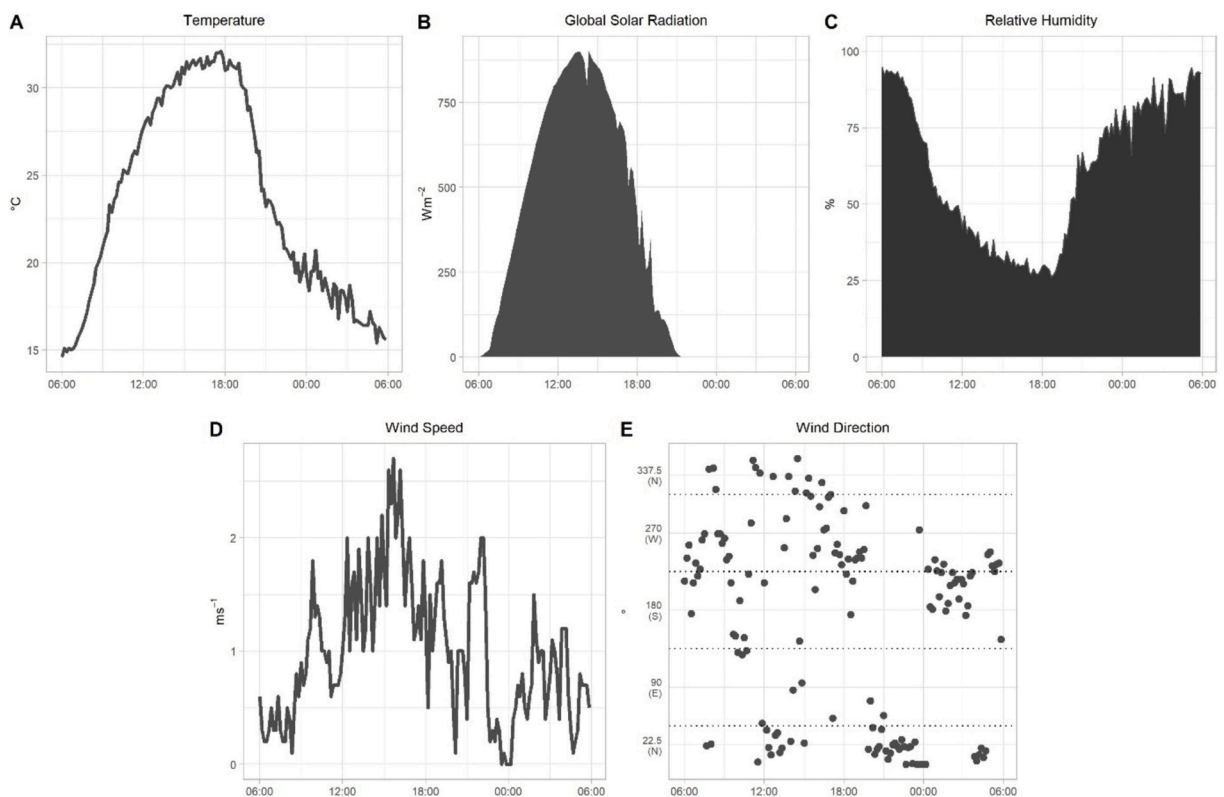


Fig. 2. Meteorological variables at the official station Bern-Zollikofen (ZOLL) from 30th July 2018, 06:00 (CEST) to 31st July 2018, 06:00 (CEST). A showing air temperature ($^{\circ}\text{C}$), B global solar radiation (Wm^{-2}), C relative humidity (%), D wind speed (ms^{-1}) and E direction of the wind ($^{\circ}$).

temperature (03:00 to 05:00 CEST, for FITNAH, MUKLIMO and PALM). While only one output file was available for LUR (22:00 to 06:00 CEST) and FITNAH (04:00 CEST), we averaged the hourly and 10 min output files from MUKLIMO and PALM for the corresponding time periods. Even though only one FITNAH output (04:00) was available, we rephrase it as “early morning temperature (03:00 to 05:00)” in the following. Second, the spatial resolution also differs from 5 m to 50 m. We therefore investigate the performance of the original resolution as well as at a 50 m averaged grid for PALM and FITNAH, which originally have a higher resolution (Table 1).

Then, we focus neither on air temperature, nor on UHI intensity, but on intra-urban air temperature variability as output variable. In previous studies (Burger et al., 2021, 2022; Burger et al., 2024), we used data of the official station ZOLL as rural reference for calculating UHI intensities. This station is located at the outer edge of the PALM domain and can therefore not be used in the present study (Fig. 1). The performance of the models would furthermore rely to a large part on the definition of a reference station, leading to high biases if the temperature of that station was modeled too high or low. To overcome this dependency, we hence define the urban air temperature variability by the difference of one station or cell to the mean of all 70 stations (for the station data), or cells where the stations are located (for the output data of the models). In the following, we will use the term “relative temperature” for this since we compare the air temperature of one station (or cell) to the mean of all other stations (or cells). For the interpretation of these relative temperatures, it has to be considered that the mean of all stations is already affected by the UHI, since most of the stations are located within the built-up area (Fig. 1).

We investigate the night from the 30th to the 31st of July 2018, since this night was modeled by LUR, MUKLIMO and PALM. However, FITNAH uses an ideal scenario with the presumption of a clear sky, a negligible mesoscale wind field and air temperature and humidity values of 21.7 °C and 50 % at 21:00 CEST at ZOLL. The conditions during that night were good, but not perfect for this scenario: The sky was mostly clear, the winds were rather weak, and air temperature and humidity reached 23.2 °C and 66.9 % at 21:00

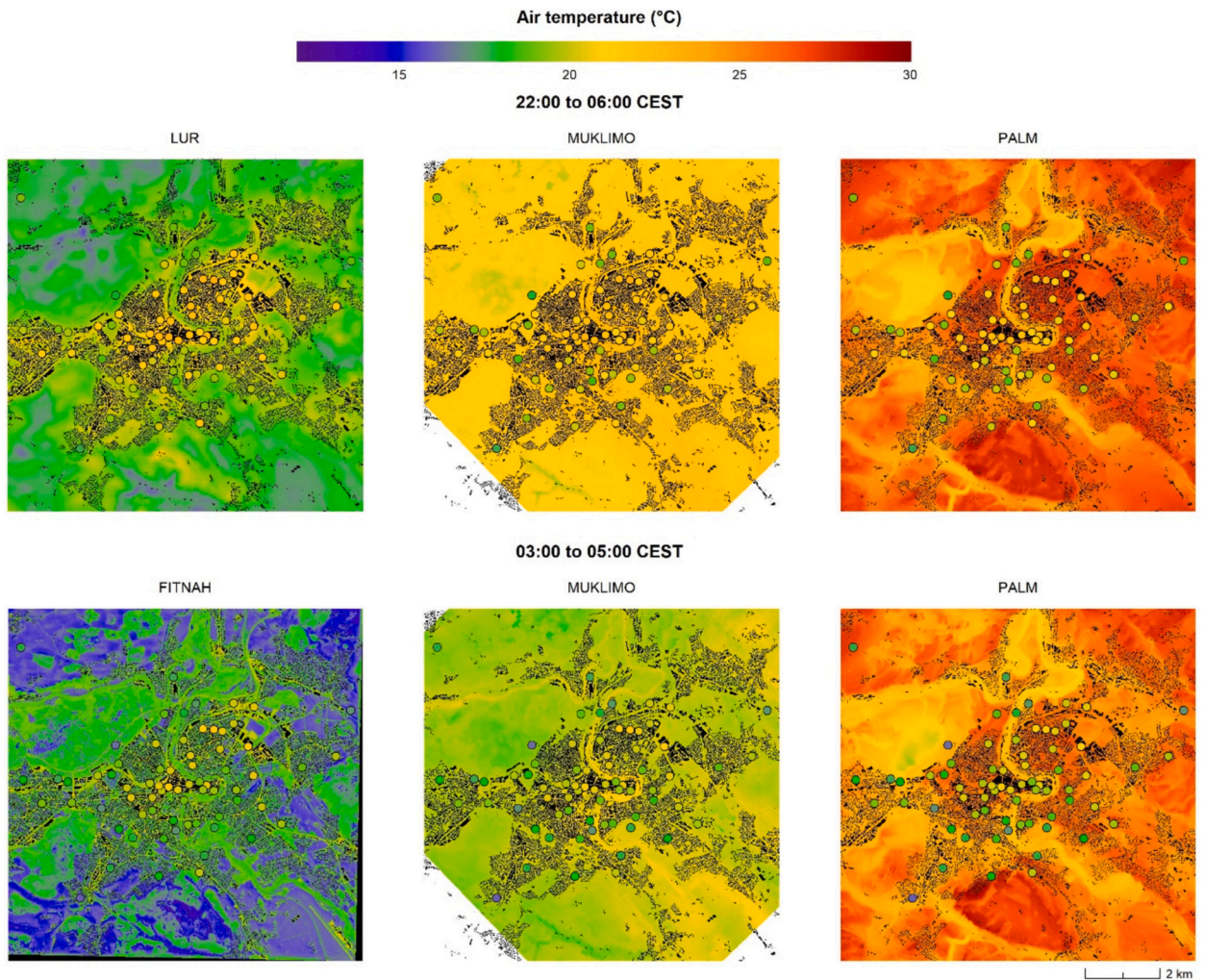


Fig. 3. Modeled air temperature of the four models compared with the measured air temperature (dots) in the night of the 30th to the 31st of July 2018. Upper row: nighttime mean from 22:00 to 06:00 CEST; lower row: early morning temperature from 03:00 to 05:00 CEST.

CEST (Fig. 2).

Additionally to that specific heat night, we simulate an ideal scenario similar to FITNAH. Therefore, we compute an average heat night, filtering all days of summer 2018 with a maximum air temperature of ≥ 25 °C, a sunshine duration of ≥ 75 %, an average wind speed of ≤ 3 ms⁻¹, and a nighttime precipitation sum of ≤ 0.3 mm. The mean of the 29 nights fulfilling these criteria was defined as the average heat night.

To investigate the model outputs regarding different urban structures, the stations were analyzed using their local climate zone (LCZ; Stewart and Oke, 2012), which were defined for the stations in Bern in an earlier study (Gubler et al., 2021). LCZs appearing only once were assigned to a similar LCZ (e.g. the only station in LCZ 1 was assigned to LCZ 2). Lastly, some differences between the model outputs are better observable if not the entire city, but a part of it is analyzed. For this, we selected a subsection of 1.5 km \times 1.5 km to be additionally analyzed (Fig. 1).

3. Results

3.1. Air temperature

Regarding modeled air temperature, large differences between the models appear (Fig. 3). The observed air temperature at the 70 stations reach a nighttime mean (22:00 to 06:00 CEST) of 20.7 °C, and an average of 19.1 °C in the early morning (03:00 to 05:00 CEST) of the 31st of July of 2018, respectively. In contrast, the mean model outputs at these locations vary from 20.1 to 25.7 °C (nighttime mean) and from 18.4 to 24.8 °C (early morning, Table 2), respectively. While LUR shows slightly lower values than the measurements, MUKLIMO and PALM overestimate the air temperature by 1.1 to 5.7 °C. FITNAH outputs show the lowest modeled temperature, but also used a 1.4 °C lower input temperature (Table S2).

3.2. Urban air temperature variability

3.2.1. Night from 30th to the 31st of July 2018 (specific heat night)

The outputs of LUR, MUKLIMO and FITNAH are dominated by blueish colors, indicating that most parts of the study region are modeled cooler than the average of the locations of the 70 measurement stations (Fig. 4). The pattern is very different, with only few red areas (relative temperature > 0 K) in MUKLIMO, some red areas in LUR, and lots of small-scale red areas mainly across streets and buildings in FITNAH. In contrast, many large red regions also outside of the city can be found in the outputs of PALM (Fig. 4). Relatively low temperatures are estimated by all models in the south of the city in a narrow valley and in the forests, although the magnitude of cooling varies markedly. Large differences appear in the Aare river valley: it is modeled very cold by PALM, slightly cold by LUR and average or even slightly warm by FITNAH and MUKLIMO (Fig. 4). The differences between the nighttime mean and the early morning temperature are small (MUKLIMO and PALM, Fig. 4).

The model performance, calculated by comparing model outputs with observed data at the location of the 70 stations, reveals that the LUR model reaches the highest correlation and the lowest RMSE (Table 3), with the scatterplot showing the best fitting distribution (Fig. 5). PALM outputs show a correlation of more than 0.6 and RMSEs of slightly above 1 K for both nighttime mean and early morning temperature. MUKLIMO outputs also show a reasonably good correlation and RMSE for the nighttime mean (Table 3). However, the scatterplot reveals a very flat distribution, showing a spread of 1.9 K between the coldest and the warmest estimate, while the observations differ by about 5.5 K for both nighttime mean and early morning temperature (Fig. 5). FITNAH shows larger RMSEs but a higher correlation than MUKLIMO for the early morning temperature. Additionally, the performance improves if 50 m averages of FITNAH are compared. Regarding PALM, the differences between the original grid (10 m) and the 50 m averages remain small (Table 3).

The analysis across the LCZs shows that relative temperatures of urban forests (LCZ A) are overestimated, and open midrise neighborhoods (LCZ 5) underestimated by all models during both time periods. In general, the relative temperature of urban green areas is mostly overestimated, except for urban parks (LCZ B) by FITNAH (Fig. 6). Large differences across the models arise in the rural surroundings, where PALM clearly overestimates, and LUR and FITNAH slightly underestimate the relative temperature. Distinct higher relative temperatures are modeled by FITNAH for the LCZ 2 (compact high-rise) and LCZ E (bare rock or paved), and by PALM for LCZ 4 (open high-rise). Additionally, LCZ BG (mix of water and urban park) is modeled markedly colder by PALM. The median bias of every LCZ is within 1 K for the LUR output (Fig. 6).

The spatial analysis shows that all models, but especially FITNAH and MUKLIMO underestimate the relative temperature in the northeastern parts of the city. The only exception is the nighttime mean output in PALM, with higher relative temperature values for half of the stations in the northeast. The relative temperature in the city center is underestimated by MUKLIMO and PALM, but slightly overestimated by FITNAH. Further, LUR, FITNAH and MUKLIMO overestimate the relative temperature in the southern and western

Table 2

Measured and modeled mean air temperature at the locations of the 70 stations in the night of the 30th to the 31st of July 2018.

Period (CEST)	Observation	LUR	MUKLIMO	PALM	FITNAH
22:00 to 06:00	20.7 °C	20.1 °C	22.1 °C	25.7 °C	–
03:00 to 05:00	19.1 °C	–	20.2 °C	24.8 °C	18.4 °C

Note: FITNAH shows the result of artificial meteorological conditions.

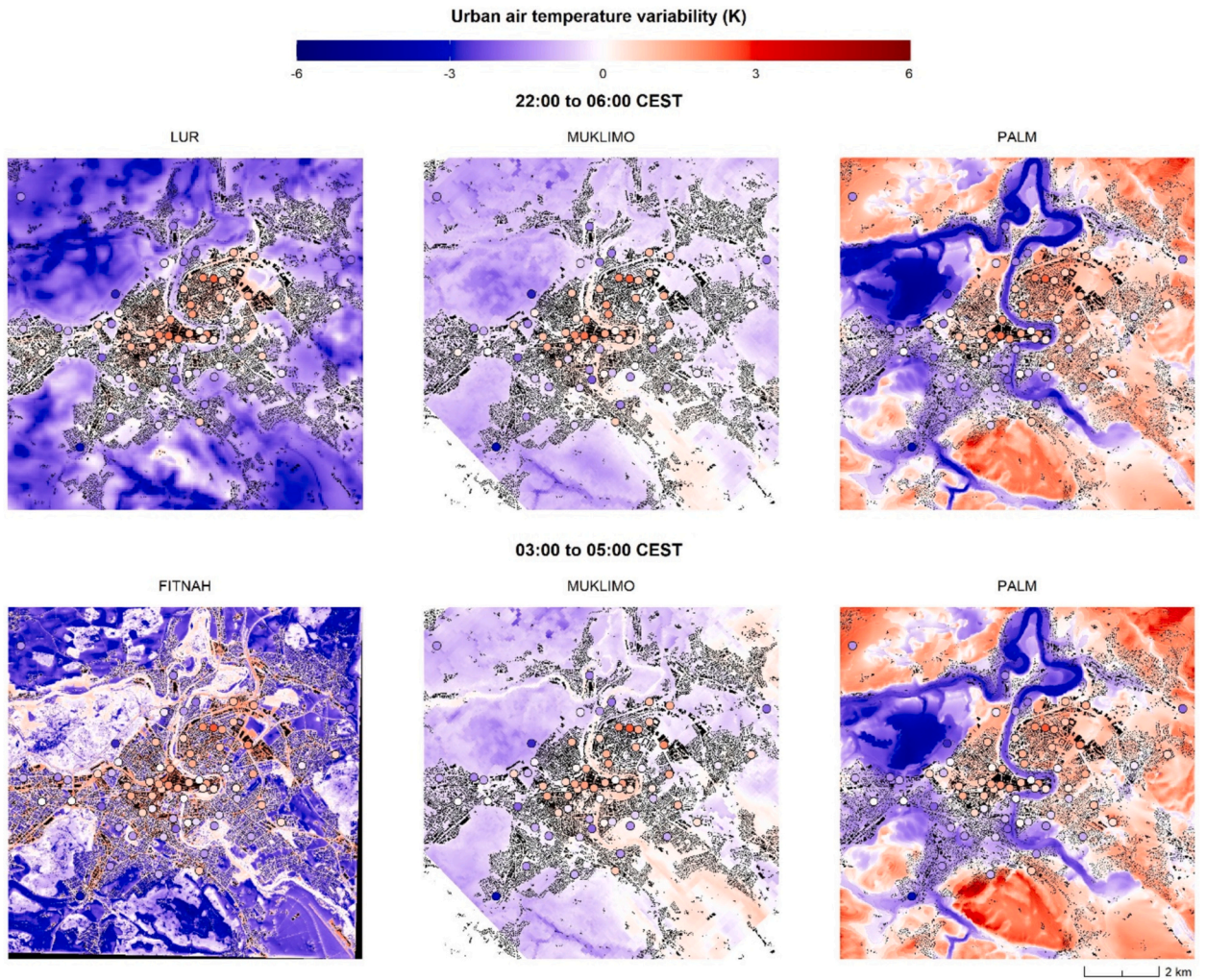


Fig. 4. Modeled urban air temperature variability across the four model outputs compared with the measured air temperature variability (dots) in the night of 30th to 31st of July 2018. Upper row: nighttime mean from 22:00 to 06:00 CEST; lower row: early morning temperature from 03:00 to 05:00 CEST.

Table 3

Statistical performance of the models compared with the station data of the night from the 30th to the 31st July of 2018. For PALM and FITNAH, the original resolution and a 50 m average are considered.

	LUR	MUKLIMO	PALM		FITNAH	
Resolution	50 m	50 m	10 m	50 m	5 m	50 m
22:00 to 06:00 CEST						
Cor	0.83	0.54	0.65	0.64	–	–
RMSE	0.73 K	1.12 K	1.04 K	1.04 K	–	–
03:00 to 05:00 CEST						
Cor	–	0.39	0.63	0.62	0.42	0.49
RMSE	–	1.12 K	1.00 K	1.02 K	1.46 K	1.29 K

Note: Cor = Correlation coefficient, RMSE = Root Mean Square Error.

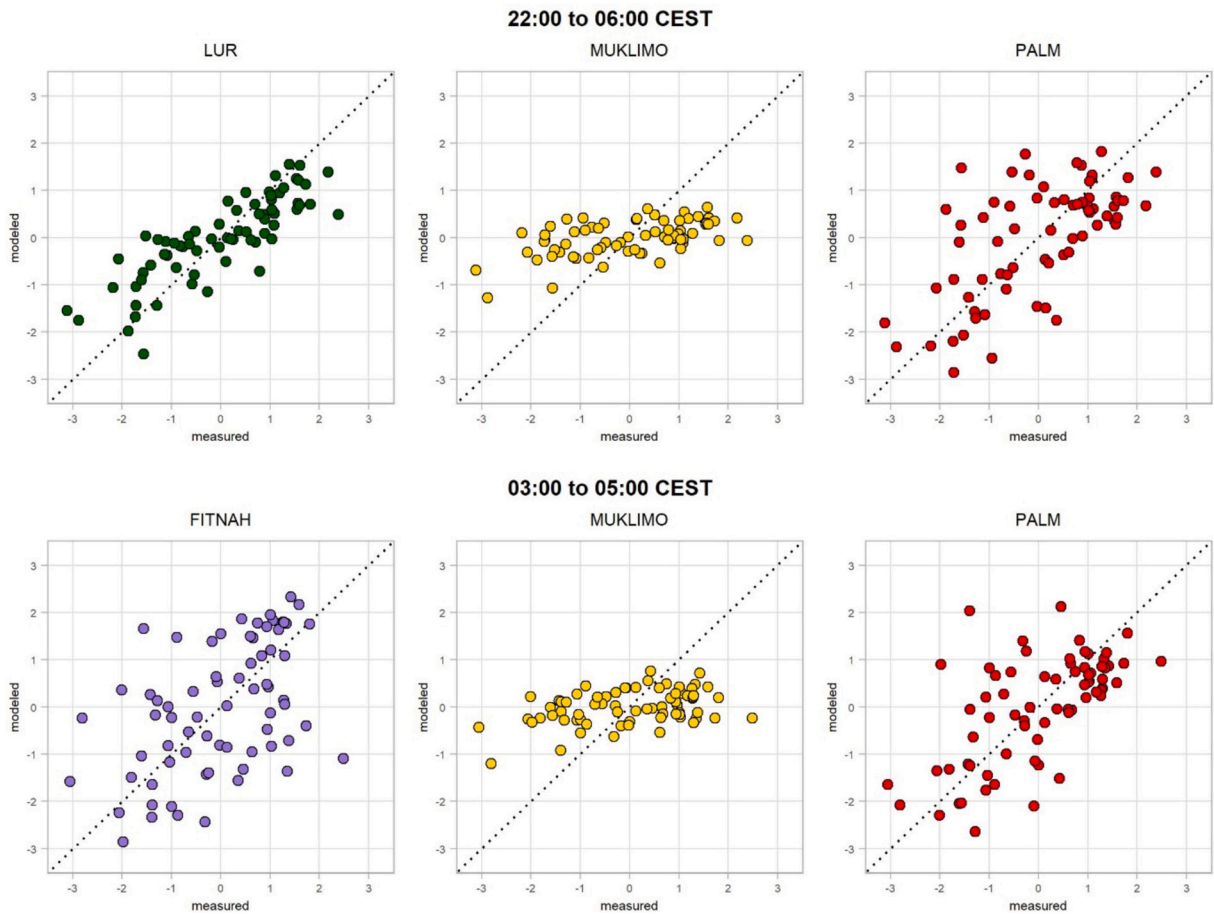


Fig. 5. Scatterplots showing the modeled urban air temperature variability (50 m averages) compared to the measured urban air temperature variability for the 70 measurement locations during the night of the 30th to the 31st July of 2018. Upper row: nighttime mean from 22:00 to 06:00 CEST; lower row: early morning temperature from 03:00 to 05:00 CEST. The statistical performance of the models can be found in [Table 3](#).

part of the city as well as in the Aare river valley (especially FITNAH and MUKLIMO). PALM tends to overestimate the relative temperature of the outskirts of Bern, especially for the nighttime mean ([Fig. 7](#)).

3.2.2. Average heat night

The comparison of the specific with the average heat night reveals that the relative temperatures were unusually high in the eastern and low in the western and southern part of the city during the night of the 30th to the 31st of July 2018 ([Fig. S1](#)). LUR, MUKLIMO and FITNAH show a better performance, when their outputs are compared to the average heat night instead of the specific heat night ([Table 3 and 4](#)). PALM shows a worse performance with a correlation being similar to that of MUKLIMO ([Table 4](#)). FITNAH shows again better results if 50 m averages are considered ([Table 4](#)). The flat distribution in the scatterplot of MUKLIMO remains similar, while FITNAH shows a rather steep distribution ([Fig. S2](#)). The performance of MUKLIMO and PALM are better for the nighttime mean than for the early morning temperature ([Table 4](#)).

The results across the LCZ and the spatial pattern of the errors remain similar, with a less pronounced west-east gradient for all models. However, the underestimation of the northeastern part still exists, especially for FITNAH and MUKLIMO ([Figs. S3 and S4](#)).

3.2.3. Small-scale analysis

The selected neighborhood for the small-scale analysis incorporates the highly built-up city center including large sealed (railway and large streets) areas, as well as the Aare river valley (in the east) and the transition to the less densely built-up area with lots of garden areas in the south of Bern ([Figs. 1 and 8](#)).

Relatively low air temperatures are modeled for the Aare river valley in PALM and LUR, but only partially in FITNAH and not at all in MUKLIMO. The built-up city center is modeled relatively warm in FITNAH and LUR, but close to average in PALM and MUKLIMO. The small green areas have a strong cooling effect in FITNAH but not in the other models. FITNAH shows overall very strong gradients between relatively warm and cold areas. These small-scale features are less pronounced in LUR and PALM and absent in MUKLIMO ([Fig. 9](#)).

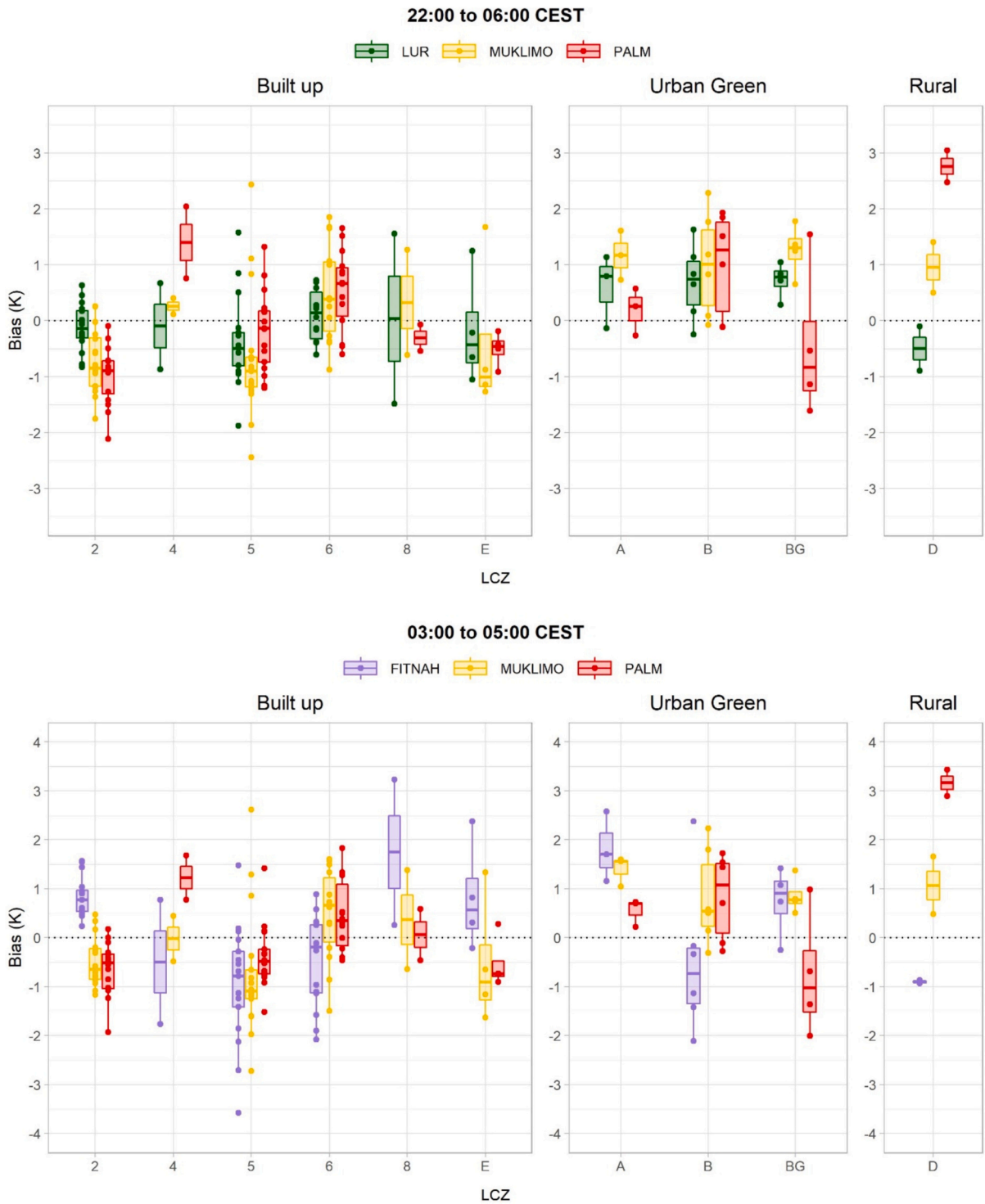


Fig. 6. Boxplots showing the bias of the modeled urban air temperature variability (50 m averages) compared to the measured urban air temperature variability for the 70 measurement locations grouped by 10 local climate zones during the night of the 30th to the 31st July of 2018. Positive values imply locations which were modeled relatively warm. The lines in the boxes show median values, the dots single stations. Upper plots: nighttime mean from 22:00 to 06:00 CEST; lower plots: early morning temperature from 03:00 to 05:00 CEST.

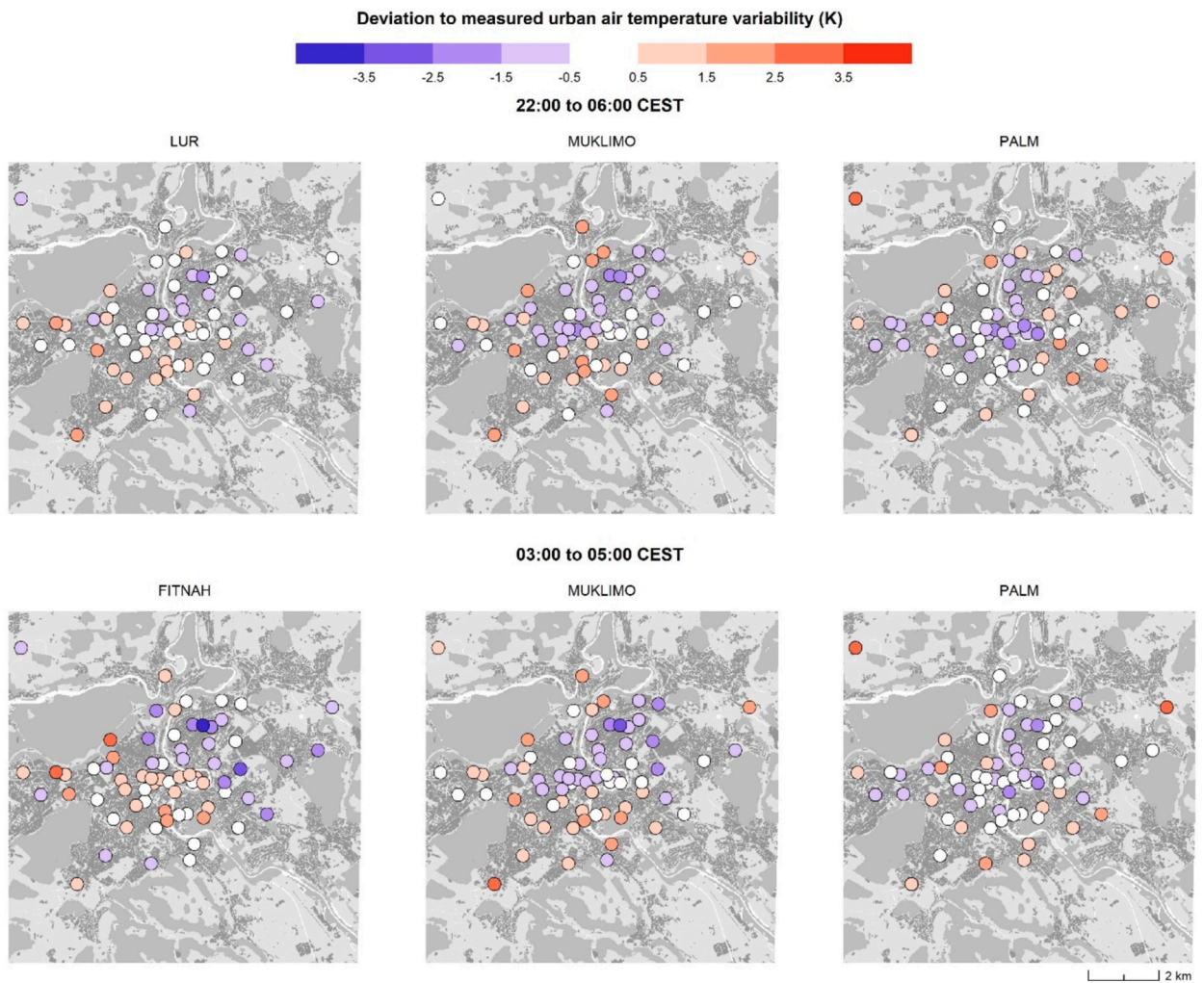


Fig. 7. Deviations from modeled (50 m averages) to measured urban air temperature variability for the 70 measurement locations in Bern during the night of the 30th to the 31st of July 2018. Blue dots mark stations where the relative temperature was modeled too low. Upper row: nighttime mean from 22:00 to 06:00 CEST; lower row: early morning temperature from 03:00 to 05:00 CEST. (For interpretation of the references to colour in this figure legend, the reader is referred to the web version of this article.)

Table 4

Statistical performance of the models compared with the mean station data of 29 heat nights in 2018. For PALM and FITNAH, the original resolution and a 50 m average are considered.

Resolution	LUR	MUKLIMO	PALM		FITNAH	
	50 m	50 m	10 m	50 m	5 m	50 m
22:00 to 06:00 CEST						
Cor	0.88	0.59	0.57	0.56	–	–
RMSE	0.50 K	0.89 K	1.05 K	1.07 K	–	–
03:00 to 05:00 CEST						
Cor	–	0.47	0.47	0.46	0.53	0.62
RMSE	–	0.76 K	1.06 K	1.06 K	1.25 K	1.06 K

Note: Cor = Correlation coefficient, RMSE = Root Mean Square Error.

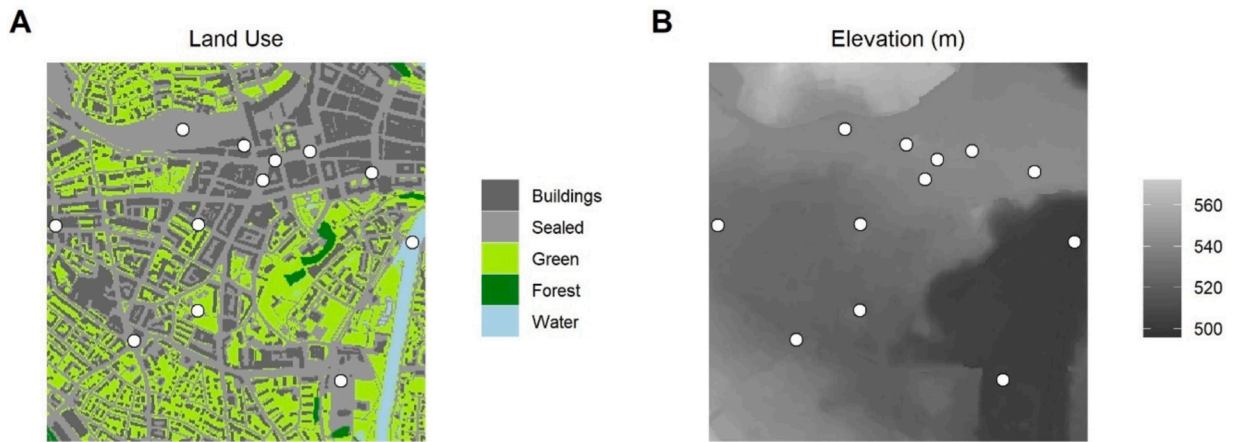


Fig. 8. Land Use (A) and Elevation (B) of the subsection including 12 measurement stations (white dots) located in that area.

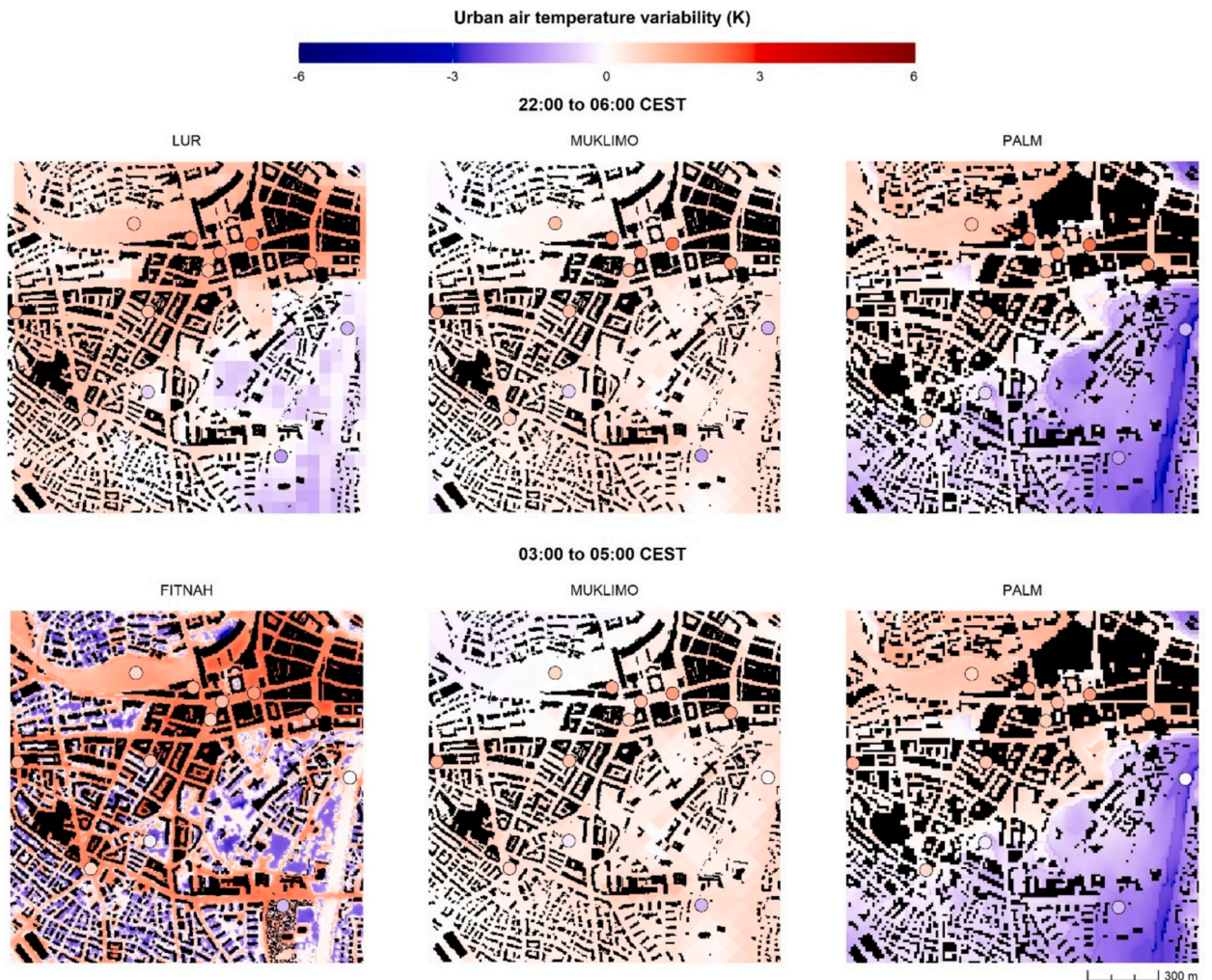


Fig. 9. Modeled and measured (dots) urban air temperature variability of the four models in the subsection. The stations show the measured urban air temperature variability in the night of the 30th to the 31st of July 2018. Upper row: nighttime mean from 22:00 to 06:00 CEST; lower row: early morning temperature from 03:00 to 05:00 CEST.

4. Discussion

The intercomparison of UCMs is challenging, since input and output data differ for every model. This might lead to very different results, which are not caused by the models themselves. For the case study of Bern, all models were using very similar spatial, but different meteorological input data (Table S1 and S2). However, the different meteorological input data used are due to varying model structures and abilities and not due to (limited) data availability. Regarding the different forms of the output data, we split the analysis in nighttime mean (22:00 to 06:00 CEST) and early morning temperature (03:00 to 05:00 CEST), analyzed a specific and an ideal average heat night, and considered the original grid spacing as well as a 50 m average as a common spatial resolution. With this set-up, we argue that a comparison of the models is viable. For the discussion of the results, we start by reviewing the differences regarding the specific and the average heat night (4.1). Then, we focus on the modeled patterns regarding urban air temperature variability (4.2) and finally discuss possible use cases of the different models (4.3).

4.1. Specific vs. average heat night

The validation of the model outputs regarding station data of a specific (night of the 30th to the 31st of July 2018) and an average (mean of 29 nights with good conditions to form urban heat) heat night revealed that LUR, FITNAH and MUKLIMO show a better performance during an average, while PALM shows a better performance during the specific heat night (Tables 3 and 4). This illustrates that the coupling with a mesoscale weather prediction model, and the exchange at the boundaries of the child and the parent domain, enables PALM to simulate specific meteorological situations. LUR and MUKLIMO also incorporate day-specific weather data (Table S2), but this data seems not to be detailed enough to reproduce the particular characteristics of a specific night, such as the higher relative temperature in the northeastern part of Bern (Fig. 7). Regarding FITNAH, the better performance for an average heat night could be expected, as the model is configured with ideal atmospheric conditions simulating a typical summer heat night.

An important feature of calm summer nights in Bern are katabatic winds from southeast, which are caused by the city's proximity to a large mountain range (Alps; Mathys et al., 1980). Although these winds are rather weak, they are important for the ventilation of the city, reaching usually the southern and the western part of Bern, but not the northeast, due to its topographic position being elevated about 70 m above the river valley (Maurer, 1976). This wind pattern was also observed during the specific heat night, showing a change in the dominant wind direction in Bern-Zollikofen at midnight (Fig. 2D and E), but only during half of the nights which were used to calculate the average heat night (14 of 29). This might explain the difference in measured air temperature variability from the specific to the average heat night (Fig. S1). Since LUR and MUKLIMO do not receive information regarding changes in meteorological variables outside of the model domain (Table 1), the information about a change in wind direction, causing a better ventilation of the southern and western part of the city, is not included in the models. This might be a reason for the underestimation of the northeastern part and the better performance during the average heat night of these models. However, also FITNAH outputs show a clear underestimation of the relative temperature in the northeast, during the specific (Fig. 7), as well as the average heat night (Fig. S4). This might indicate that exchange with the wind field outside of the domain is too weak and the presumption of negligible winds for the city of Bern is too strong.

4.2. Urban air temperature variability outputs of four different models

The shape of the UHI varies substantially between the different models (Figs. 4 and 9). MUKLIMO shows a very narrow temperature spread for the modeled night. The pattern of only low nighttime UHI intensities was observed during all heatwaves simulated in Bern (Hürzeler et al., 2022). As main reasons for that result, the spatial resolution of 50 m, unresolved buildings and vague information about the initial boundary conditions (vertical profile at only two locations; estimated soil moisture and soil temperature; Table S2) have been identified (Hürzeler et al., 2022). Other studies found larger nighttime maximum UHI intensities modeled by MUKLIMO (between 5 and 6.4 K; Bokwa et al., 2019), but also similar findings with very small UHI intensities exist (Geletić et al., 2016). The homogenous air temperature distribution of MUKLIMO thus leads to an underestimation of locations with high relative temperatures and an overestimation of locations with low relative temperatures, respectively (Fig. 6).

The outputs of the FITNAH model show strong small-scale temperature gradients and an overall heterogeneous shape of the UHI of Bern (Fig. 4). The analysis reveals that small green areas within the city show similarly low relative temperatures than larger green areas in the rural surroundings (Fig. 4). A closer look to the subsection (Figs. 8 and 9) furthermore indicates that the model outputs of FITNAH follow the land use / cover data, with sealed areas showing high, and green areas showing low relative temperatures. However, the LCZ-based analysis reveals that these temperature gradients are rather overestimated by FITNAH since the relative temperatures are overestimated for sealed areas (LCZ 2 and E) and underestimated for green urban areas (LCZ B).

In the PALM model outputs, the most prominent feature shaping the UHI of Bern are cold air streams, which are only barely visible in the outputs of MUKLIMO and FITNAH. Topographic depressions (e.g. Aare river valley) are modeled to be cold, whereas hilltops and slopes are modeled to be warm (Figs. 1, 4 and 9). Due to cold air streams being more important in the southwestern part of Bern, the shape of the UHI is shifted towards the northeastern part of the city, which is in line with the measurements (Fig. 4). However, the high relative temperatures of the rural surroundings lead to a UHI pattern that is not showing the usual urban-rural temperature gradient (Fig. 4). The LCZ-based analysis reveals that the relative temperatures of the two rural stations (LCZ D) are indeed modeled far too high, while the relative temperatures of the stations in the Aare river depression (LCZ BG; green and water) are rather modeled too low. Hence, the effect of topography might be overestimated, and the effect of land use (LCZ 2 and E rather too cool; LCZ B too warm) underestimated (Fig. 8) in the PALM outputs, which contrasts with the FITNAH outputs. An example for different parameterization of

topography of these two models can be observed along the Gurten hill south of Bern, which is modeled by FITNAH to be cold and by PALM to be warm (Fig. 4). A short-term measurement campaign in summer 2021 showed that temperature inversions during typical warm nights may indeed lead to air temperatures being even higher on the hilltop than in the city center (Baer, 2023).

Finally, the LUR outputs show a combination of land use and topographic features, leading to a more typical UHI pattern with high relative temperatures for strongly sealed areas of Bern and low relative temperatures for large green areas and topographic depressions (Figs. 4 and 9). The outputs from the LUR model show the best statistical performance (Tables 3 and 4, Fig. 5) and a good representation of all urban structures, with a median error smaller than 1 K across all LCZs (Figs. 6 and S3). In general, the relative temperatures of urban green areas are slightly overestimated, which might be due to the large buffer radii (of up to 1000 m) used, which may impede the adequate modeling of cooling effects of small inner-city green areas (Burger et al., 2022). Regarding the comparability of the models, it is important to mention that 49 out of the 70 stations used for validation were previously used to calibrate the LUR model (in the years 2018 to 2020; Burger et al., 2022). The validation of the LUR model showed similar results for the subsequent years of 2021 and 2022 and stations not used for validation, but a certain advantage of the LUR in comparison to numerical models can nevertheless be stated.

4.3. Spoilt for choice: which model to choose?

The air temperature outputs of four models applied to the same city show very different results ranging from modeling only weak intra-urban temperature variabilities (MUKLIMO) to strong small-scale temperature gradients within neighborhoods (FITNAH, Figs. 3, 4 and 9). This confirms that validation with in-situ data is crucial, especially since output users might not be aware of the limitations of a certain modeling approach. We therefore encourage modelers to validate the model at least with some additional in-situ measurements to enhance the confidence level of the applied models.

The outputs of MUKLIMO show good results regarding air temperature in the highly built-up area of Bern (Fig. 3). However, the spatial extent of the UHI is largely overestimated, leading in too high air temperatures in the rural surroundings, and thus to too little urban air temperature variability (Fig. 4; Hürzeler et al., 2022). The performance of MUKLIMO could possibly be improved with more detailed meteorological input parameters, but since they are not available for Bern, an improvement is difficult to realize. Nevertheless, the correlation for the nighttime mean of the average heat night reaches 0.59 (Table 4), which shows that hot and cool spots of an average night can be detected by MUKLIMO, while an estimation of the UHI magnitude in a topographic complex and rather small city remains difficult.

If data from an air temperature measurement network is available, LUR can be used to derive nighttime urban air temperature maps at high quality and with a low amount of computational and financial resources (Burger et al., 2022). However, for city administrations, the effort to establish and operate such a network is crucial. Therefore, the question arises how much data (number of stations and duration of operation) is needed to calculate a coherent LUR, and whether such models can be transferred from one city to another. To estimate the potential of LUR approaches regarding urban heat island mapping in general, these questions should be addressed in future research.

The coupling of different domains with a mesoscale model enables the simulation of realistic meteorological scenarios and the modeling of large-scale ventilation patterns with PALM. Only PALM outputs reproduce the elevated air temperature for the north-eastern part of the city and show a better performance during the specific heat night (Tables 3 and 4; Figs. 4 and 7). However, air temperatures of rural areas are clearly overestimated, with partly even higher values than in the city center, resulting in a weak modeled overall UHI (Figs. 4 and 6). Additionally, a large positive bias, reaching up to 5 K is observed (Table 2 and Fig. 3). A similar pattern of PALM estimating too high air temperatures at night was also found in two validation studies in Prague, with maximum differences reaching 2.5 K (Resler et al., 2021; Geletič et al., 2021). This bias was mainly explained by insufficient cooling near the surface, due to atmospheric conditions modeled not stable enough (Resler et al., 2021). In the present study, the height of the analyzed layer (5 m instead of 3 m; Table 1) and too warm boundary conditions (induced by the parent domain and COSMO-1) might have led to that even larger bias. However, we sum up that if a specific scenario of a city with complex topography and ventilation scheme is investigated, PALM is a good option to analyze the urban air temperature variability.

Lastly, the FITNAH output represents the urban air temperature variability in the early morning (03:00 to 05:00 CEST) of an average heat night with a correlation of 0.53 to 0.62 (Table 4), which is the best performance for that period. Interestingly, the performance of the model is better if an averaged 50 m grid, and not the original grid of 5 m is analyzed (Tables 3 and 4). This might indicate that the large air temperature variability within small areas is overestimated by the 5 m outputs of FITNAH (Fig. 9). Additionally, it has been shown, that air temperature differences induced by land use dominate the outputs of FITNAH, leading to a slight overestimation of mainly sealed areas and a highly fragmented overall UHI (Figs. 6 and 10). Following from that, and due to the set-up of modeling an ideal meteorological situation, we suggest that FITNAH is well suited as a basis for urban planning purposes of cities, which air temperature distribution are primary dominated by land use patterns.

Finally, we would like to point out that we only focused on nighttime air temperature outputs of a specific and an average heat night during summer in the present study. The intra-urban temperature gradients are usually the strongest, and people are constrained to stay at their place of residence during the night, which makes the analysis of urban nighttime temperatures of great importance (Theeuwes et al., 2017; Burger et al., 2021). However, modeling with MUKLIMO, FITNAH and PALM would also enable the analysis of other urban climate variables such as wind fields, cold air accumulations or daytime air temperature and corresponding indices (e.g. physiologically equivalent temperature). Conversely, the LUR dataset presented here would also include urban temperature maps of rainy or windy nights, which are usually not simulated with PALM, FITNAH or MUKLIMO (Hürzeler et al., 2022; Burger et al., 2024). Although not discussed here, the potential of a model to simulate different urban climate variables or varying meteorological

conditions might be as well important for model users concerning their selection of the desired urban climate model.

5. Conclusion

In this study, we compared nighttime air temperature variability modeled by a land use regression (LUR) and three numerical urban climate models (FITNAH 3D, MUKLIMO_3 and PALM) with station data from 70 locations in the city of Bern, Switzerland. Our main findings are the following:

- MUKLIMO_3 outputs clearly underestimate the urban air temperature variability of Bern.
- PALM outputs show a strong positive bias. Regarding urban air temperature variability, it is the only model, which shows a better performance regarding a specific and not an average heat night, due to the coupling with a mesoscale weather forecast model.
- FITNAH 3D outputs reach a good correlation with the measured average values of all heat nights in a summer. Land use patterns are the most important urban features influencing the output of the model.
- LUR outputs show the highest correlation (0.83 to 0.88) and a lowest RMSE (0.50 to 0.73 K) across all models. If detailed air temperature data is available in a city, LUR is a good method to model urban air temperature variability.

In general, the outputs vary substantially between the models. If they are applied for practical use, validation with in-situ measurements is key to enhance the confidence level of the modeled data. Additionally, the limitations of the applied model should be discussed by the modelers, especially when providing reports to city administrations for urban planning purposes.

Supplementary data to this article can be found online at <https://doi.org/10.1016/j.uclim.2024.102166>.

Author statement

The authors declare that they have all seen and approved the final version of the manuscript and that the article has not received prior publication and is not under consideration for publication elsewhere.

Moritz Burger, Moritz Gubler, Achim Holtmann, Stefan Brönnimann.

Funding information

This project is funded by a grant of the Oeschger Centre for Climate Change Research (OCCR) and the FAIRNESS (FAIR NETwork of micrometeorological measurements, CA20108) project.

CRedit authorship contribution statement

Moritz Burger: Writing – review & editing, Writing – original draft, Visualization, Validation, Software, Resources, Methodology, Investigation, Formal analysis, Data curation, Conceptualization. **Moritz Gubler:** Writing – review & editing, Conceptualization. **Achim Holtmann:** Writing – review & editing, Software, Methodology, Data curation. **Stefan Brönnimann:** Writing – review & editing, Supervision, Funding acquisition, Conceptualization.

Declaration of competing interest

The authors declare that they have no known competing financial interests or personal relationships that could have appeared to influence the work reported in this paper.

Data availability

Data will be made available on request.

Acknowledgements

We thank Cornelia Burmeister and Dirk Pavlik from GEO-NET Umweltconsulting GmbH for providing the FITNAH 3D data for Bern and for the discussion of the results. We also thank Michael Schmutz from Meteotest AG for the modeling of PALM and for his assistance regarding the handling of the output data and the description of the input data. We furthermore thank André Hürzeler for his help regarding the MUKLIMO_3 data. We finally thank the city of Bern and Energie Wasser Bern for their support regarding the measurement network in Bern.

References

- Baer, S., 2023. Analyse Und Modellierung von Kaltluft Im Aaretal der Stadt Bern (EN: "Analysis and Modeling of Cold Air in the Aare Valley in the City of Bern"). Master thesis. University of Bern, p. 58p.

- Bokwa, A., Geletić, J., Lehnert, M., Žuvela-Aloise, M., Hollósi, B., Gál, T., Skarbit, N., Dobrovolný, P., Hajto, M.J., Kielar, R., Walawender, J.P., Štátný, P., Holec, J., Ostapowicz, K., Burianová, J., Garaj, M., 2019. Heat load assessment in central European cities using an urban climate model and observational monitoring data. *Energ. Buildin.* 201, 53–69.
- Bundesamt für Statistik (BFS), 2022. Ständige Wohnbevölkerung nach Staatsangehörigkeitskategorie, Geschlecht und Gemeinde, definitive Jahresergebnisse 2021 EN: “Permanent Resident Population by Citizenship Category, Gender, and Municipality, Final Annual Results 2021”. Published: 25.08.2022. BFS Nummer: su-d-01.02.03.01.01.
- Bundo, M., de Schrijver, E., Federspiel, A., Toreti, A., Xoplaki, E., Luterbacher, J., Franco, O.H., Müller, T., Vicedo-Cabrera, A.M., 2021. Ambient temperature and mental health hospitalizations in Bern, Switzerland: A 45-year time-series study. *PLoS One* 16 (10), e0258302.
- Burger, M., Gubler, M., Heinemann, A., Brönnimann, S., 2021. Modelling the spatial pattern of heatwaves in the city of Bern using a land use regression approach. *Urban Clim.* 38, 100885.
- Burger, M., Gubler, M., Brönnimann, S., 2022. Modeling the intra-urban nocturnal summertime air temperature fields at a daily basis in a city with complex topography. *PLoS Climate* 1 (12), e0000089.
- Burger, M., Gubler, M., Brönnimann, S., 2024. High-resolution dataset of nocturnal air temperatures in Bern, Switzerland (2007–2022). *Geosci. Data J.* 00, 1–15.
- Erlwein, S., Zölch, T., Pauleit, S., 2021. Regulating the microclimate with urban green in densifying cities: joint assessment on two scales. *Build. Environ.* 205, 108233.
- Foissard, X., Dubreuil, V., Quénot, H., 2019. Defining scales of the land use effect to map the urban heat island in a mid-size European city: Rennes (France). *Urban Clim.* 29, 100490.
- García-León, D., Casanueva, A., Standardi, G., Burgstall, A., Flouris, A.D., Nybo, L., 2021. Current and projected regional economic impacts of heatwaves in Europe. *Nat. Commun.* 12 (1), 5807.
- Geletić, J., Lehnert, M., Dobrovolný, P., 2016. Modelled spatio-temporal variability of air temperature in an urban climate and its validation: a case study of Brno, Czech Republic. *Hungar. Geogr. Bull.* 65 (2), 169–180.
- Geletić, J., Lehnert, M., Krč, P., Resler, J., Krayenhoff, E.S., 2021. High-resolution modelling of thermal exposure during a hot spell: A case study using PALM-4U in Prague, Czech Republic. *Atmosphere* 12 (2), 175.
- GEO-NET, 2018. Analyse der klimaökologischen Funktionen Und Prozesse für das Gebiet Des Kantons Zürich (EN: “Analysis of Climate-Ecological Functions and Processes for the Area of the Canton of Zurich”). Report on Behalf on the Building Direction of the Canton of Zurich, Hannover, p. 98.
- GEO-NET, 2020. Situation Climat-Écologique Due Canton de Genève: Analyse Climatologique sur la Base d’un Modèle (EN: “Climate-Ecological Situation in the Canton of Geneva: Model-Based Climate Analysis”). Report on Behalf of the Republic and Canton on Geneva, Hannover, p. 83.
- GEO-NET, 2023. Klimaökologische Situation der Stadt Bern: Modellbasierte Klimaanalyse (EN: “Climate-ecological situation of the city of Bern: Model-Based Climate Analysis. Final Report”). Report on Behalf on the City of Bern, Hannover, p. 65.
- Gross, G., 1992. Results of supercomputer simulations of meteorological mesoscale phenomena. *Fluid Dynami. Res.* 10 (4–6), 483.
- Gubler, M., Christen, A., Remund, J., Brönnimann, S., 2021. Evaluation and application of a low-cost measurement network to study intra-urban temperature differences during summer 2018 in Bern, Switzerland. *Urban Clim.* 37, 100817.
- Heus, T., van Heerwaarden, C.C., Jonker, H.J., Pier Siebesma, A., Axelsen, S., Van Den Dries, K., Geoffroy, O., Moene, A.F., Pino, D., de Roode, S.R., Vilà-Guerau de Arellano, J., 2010. Formulation of the Dutch atmospheric large-Eddy simulation (DALES) and overview of its applications. *Geosci. Model Dev.* 3 (2), 415–444.
- Hoek, G., Beelen, R., De Hoogh, K., Vienneau, D., Gulliver, J., Fischer, P., Briggs, D., 2008. A review of land-use regression models to assess spatial variation of outdoor air pollution. *Atmos. Environ.* 42 (33), 7561–7578.
- Hürzeler, A., Hollósi, B., Burger, M., Gubler, M., Brönnimann, S., 2022. Performance analysis of the urban climate model MUKLIMO_3 for three extreme heatwave events in Bern. *City Environ. Interact.* 16, 100090.
- Jerrett, M., Arain, A., Kanaroglou, P., Beckerman, B., Potoglou, D., Sahuvaroglu, T., Morrison, J., Giovis, C., 2005. A review and evaluation of intraurban air pollution exposure models. *J. Expo. Sci. Environ. Epidemiol.* 15 (2), 185–204.
- Maronga, B., Gryschka, M., Heinze, R., Hoffmann, F., Kanani-Sühring, F., Keck, M., Ketelsen, K., Letzel, M.O., Sühring, M., Raasch, S., 2015. The parallelized large-Eddy simulation model (PALM) version 4.0 for atmospheric and oceanic flows: model formulation, recent developments, and future perspectives. *Geosci. Model Dev.* 8 (8), 2515–2551.
- Maronga, B., Banzhaf, S., Burmeister, C., Esch, T., Forkel, R., Fröhlich, D., Fuka, V., Gehrke, K.F., Geletić, J., Giersch, S., Gronemeier, T., Groß, G., Heldens, W., Hellsten, A., Hoffmann, F., Inagaki, A., Kadasch, E., Kanani-Sühring, F., Ketelsen, K., Khan, B.A., Knigge, C., Knoop, H., Krč, P., Kurppa, M., Maamari, H., Matzarakis, A., Mauder, M., Pallasch, M., Pavlik, D., Pfäfferott, J., Resler, J., Rissmann, S., Russo, E., Salim, M., Schrempf, M., Schwenkel, J., Seckmeyer, G., Schubert, S., Sühring, M., von Tils, R., Vollmer, L., Ward, S., Witha, B., Wurps, H., Zeidler, J., Raasch, S., 2020. Overview of the PALM model system 6.0. *Geosci. Model Dev.* 13 (3), 1335–1372.
- Mathys, H., Maurer, R., Messerli, B., Wanner, H., Winiger, M., 1980. Klima und Lufthygiene im Raum Bern. Resultate des Forschungsprogramms KLIMUS und ihre Anwendung in der Raumplanung (EN: “climate and air pollution control in the area of Bern. Results of the KLIMUS research program and the application in urban planning”). *Schweizerische Naturforschende Gesellschaft* 40 (7), S., Bern.
- Maurer, R., 1976. Das Regionale Windgeschehen (EN: “The Regional Wind Pattern”). Beiträge zum Klima der Region Bern. Geographisches Institut der Universität Bern, Bern.
- Meteotest, 2020. Stadtklimaanalyse St. Gallen. Modellierung der Hitzebelastung und der Durchlüftung (EN: “Urban Climate Analysis St. Gallen. Modeling of Heat Load and Ventilation”). Requested by the City of St.Gallen. Bern, p. 30.
- Mishra, V., Ganguly, A.R., Nijssen, B., Lettenmaier, D.P., 2015. Changes in observed climate extremes in global urban areas. *Environ. Res. Lett.* 10 (2), 024005.
- Muller, C.L., Chapman, L., Grimmond, C.S.B., Young, D.T., Cai, X., 2013. Sensors and the city: a review of urban meteorological networks. *Int. J. Climatol.* 33 (7), 1585–1600.
- Oke, T.R., Mills, G., Christen, A., Voogt, J.A., 2017. *Urban climates*. Cambridge University Press.
- Oswald, S.M., Hollósi, B., Žuvela-Aloise, M., See, L., Guggenberger, S., Hafner, W., Prokop, G., Storch, A., Schieder, W., 2020. Using urban climate modelling and improved land use classifications to support climate change adaptation in urban environments: A case study for the city of Klagenfurt, Austria. *Urban Clim.* 31, 100582.
- Resler, J., Eben, K., Geletić, J., Krč, P., Rosecký, M., Sühring, M., Belda, M., Fuka, V., Halenka, T., Huszár, P., Karlický, J., Benešová, N., Döbaldová, J., Honzáková, K., Keder, J., Nápravníková, Š., Vlček, O., 2021. Validation of the PALM model system 6.0 in a real urban environment: A case study in Dejvice, Prague, the Czech Republic. *Geosci. Model Dev.* 14 (8), 4797–4842.
- Rizwan, A.M., Dennis, L.Y., Chunho, L.I.U., 2008. A review on the generation, determination and mitigation of Urban Heat Island. *J. Environ. Sci.* 20 (1), 120–128.
- Sievers, U., 2012. Das Kleinskalige Strömungsmodell MUKLIMO_3 Teil 1: Theoretische Grundlagen, PC-Basisversion Und Validierung (EN: “The Small-Scale Flow Model MUKLIMO 3 Part 1: Theoretical Foundations, Basic PC Version and Validation”). Selbstverlag Des Deutschen Wetterdienstes. Offenbach am Main.
- Sievers, U., 2016. Das kleinskalige Strömungsmodell MUKLIMO 3. Teil 2: Thermodynamische Erweiterungen (EN: “The small-scale flow model MUKLIMO_3. Part 2: Thermodynamic extensions”). Selbstverlag Des Deutschen Wetterdienstes. Offenbach am Main.
- Stewart, I.D., Oke, T.R., 2012. Local climate zones for urban temperature studies. *Bull. Am. Meteorol. Soc.* 93 (12), 1879–1900.
- Theeuwes, N.E., Steeneveld, G.J., Ronda, R.J., Holtlag, A.A., 2017. A diagnostic equation for the daily maximum urban heat island effect for cities in northwestern Europe. *Int. J. Climatol.* 37 (1), 443–454.
- UN (United Nations), Department of Economic and Social Affairs, Population Division, 2019. *World Urbanization Prospects: The 2018 Revision (ST/ESA/SER.A/420)*. United Nations, New York.
- van der Linden, L., Hogan, P., Maronga, B., Hagemann, R., Bechtel, B., 2023. Crowdsourcing air temperature data for the evaluation of the urban microscale model PALM - A case study in Central Europe. *PLOS Climate* 2 (8), e0000197.
- Vicedo-Cabrera, A.M., Scovronick, N., Sera, F., Roye, D., Schneider, R., Tobias, A., Astrom, C., Guo, Y., Honda, Y., Hondula, D.M., Abrutzky, R., Tong, S., Coelho, M.D.Z.S., Saldiva, P.H.N., Lavigne, E., P.M., Correa, P.M., Ortega, N.V., Kan, H., Osorio, S., Kysely, J., Urban, A., Orru, H., Indermitte, E., Jaakkola, J.J.K., Rytty, N.,

- Pascal, M., Schneider, A., Katsouyanni, K., Samoli, E., Mayvaneh, F., Entezari, A., Goodman, P., Zeka, A., Michelozzi, P., de' Donato, F., Hashizume, M., Alahmad, B., Diaz, M.H., Valencia, C.D., Overcenco, A., Houthuijs, D., Ameling, C., Rao, S., Di Ruscio, F., Carrasco-Escobar, G., Seposo, X., Silva, S., Madureira, J., Holobaca, I.H., Fratianni, S., Acquaforte, F., Kim, H., Lee, W., Iniguez, C., Forsberg, B., Ragettli, M.S., Guo, Y.L.L., Chen, B.Y., Li, S., Armstrong, B., Aleman, A., Zanobetti, A., Schwartz, J., Dang, T.N., Dung, D.V., Gillett, N., Haines, A., Mengel, M., Huber, V., Gasparrini, A., 2021. The burden of heat-related mortality attributable to recent human-induced climate change. *Nat. Clim. Change* 11 (2021), 492–500.
- Vogel, J., Afshari, A., Chockalingam, G., Stadler, S., 2022. Evaluation of a novel WRF/PALM-4U coupling scheme incorporating a roughness-corrected surface layer representation. *Urban Clim.* 46, 101311.
- WMO (World meteorological organization), 2021. Guide to Instruments and Methods of Observation. Volume III - Observing Systems. 2021 edition. WMO-No. 8. Geneva.